Pulse Asymptotics of the Charney Baroclinic Instability Problem

BRIAN F. FARRELL

Center for Earth and Planetary Physics, Harvard University, Cambridge, MA 02138

(Manuscript received 16 July 1981, in final form 13 October 1981)

ABSTRACT

The asymptotic response of the Charney baroclinic instability problem to a localized perturbation is determined using the formalism of Briggs (1964) and exploiting a recently obtained highly accurate WKB approximate dispersion relation (Lindzen and Rosenthal, 1981). Comparison is made with previous results for two-level and Eady models.

Small scales and rapid growth characteristic of the initial stages of cyclogenesis are found and the linear dispersion relation, which can be obtained from observation of zonal wind and stability, emerges as a forecast tool for prediction of geographically local cyclogenesis.

1. Introduction

Since its discovery in the work of Charney (1947) and Eady (1949), baroclinic instability has been accepted as a major source of synoptic-scale disturbances in midlatitudes. The normal-mode method of analysis used in these early works and in most subsequent investigations makes the assumption of a solution infinitely periodic in the horizontal direction and determines the space-independent growth rate as an eigenvalue of the resulting system of equations. The wavelength of the disturbance most rapidly growing in time is then compared with observed synoptic cyclone scales. The agreement found encourages the identification of these features with baroclinic instability. However, this identification requires that the response of the baroclinically unstable fluid to an initial perturbation, which is most likely localized in space, will evolve into normal mode form. Whether this happens can be decided within the restrictions of linear theory by solving the appropriate initial value problem. In the case investigated here it is found that as a function of distance from the initial perturbation, widely different space scales dominate the solution, calling into question the identification of maximally time-growing normal mode wavenumber with the scale of synoptic features.

As it is usually formulated, the IVP requires finally the double inversion of a Fourier transform in space and a Laplace transform in time; in general a formidable task even for the simplest of models. Progress has been made in the asymptotic evaluation of these integrals for large time, in work done in connection with plasma instabilities (Briggs, 1964). It is found that this limit is determined by the linear dispersion relation generalized to complex frequency and wavenumber. An important conceptual distinction is pointed out by the analysis—that between the so-called absolute and convective instabilities. In the former the response continues to grow in time at every point which has been reached by the traveling pulse; in particular, it continues to grow at the point of excitation. In the latter the instability is carried along with the flow so that despite its constantly increasing amplitude, at any fixed point the disturbance eventually decreases; in particular, at the point of the excitation the effects of perturbation are eliminated after finite time.

Absolute instability has been found for sufficiently small shear in the two-layer model on an f-plane and on the β-plane (Merkine, 1980). The Eady problem was examined by Simmons and Hoskins (1979) and found to have no absolute instability. These model flows have the virtue of possessing dispersion relations expressible in simple analytic form, but are limited in that the structure of these dispersion relations, which is of less consequence in picking out most rapidly growing in time normal modes, is crucial to the asymptotics of pulses. In the hierarchy of baroclinic models the Charney problem is the simplest one to possess at least in modified form most of the features of realistic dispersions from global models (Simmons and Hoskins, 1976; Geisler and Garcia, 1977). Unfortunately, the solution of the Charney model is in terms of hypergeometric functions and yields no exact closed form dispersion relation. In what follows, a highly accurate approximate dispersion relation is used to extend pulse asymptotic results to this case.

It should be borne in mind that these linear asymptotics are valid only after an unspecified long time has elapsed since the original perturbation; it is possible that for some initial conditions the entire development to nonlinear equilibration of the system which is being modeled may take place before these

0022-4928/82/030507-11$06.75

results obtain validity. The time scale for evolution of an initial barotropic perturbation to normal mode form in a baroclinic zonal flow is examined in a forthcoming report (Farrell, 1981). That it may be comparable to synoptic time scales is indicated by the slow approach to normal mode form exhibited by the pulse-excited Eady example in Simmons and Hoskins (1979).

2. Method of analysis

The initial value solution is an integral over the normal mode solutions consisting of the exponentially growing modes and their complex conjugate decaying modes plus another integral over a continuous spectrum. The decaying exponentials make no contributions to the long time behavior and the continuous spectrum contributes at most $O(t)$ (Burger, 1966), so the asymptotic solution takes the form of an integral over the exponentially growing modes

$$\psi(x, z, t) = \int_{-\infty}^{\infty} dk a(k)\psi_k(z)e^{i[kx/t-\omega(k)]t}, \quad (1)$$

where $a(k)$ is the projection of initial conditions on the normal mode at k and $\psi_k(z)$ the vertical structure of mode at k. Let

$$\Omega(k) = -\left[k\frac{x}{t} - \omega(k)\right].$$

Evaluation of (1) is carried out for a frame of reference moving at speed $U = x/t$ by deforming the path of integration in the k plane in the direction of diminishing Ω_i until one of two conditions is met:

1) There is reached a contour for which $\Omega_i \leqslant 0$ for all k without having encountered a point k_s where

$$\left.\frac{\partial\Omega}{\partial k}\right|_{k_s} = 0 \quad \text{and} \quad \Omega_i > 0,$$

in which case the system is stable as viewed from the translating frame.

2) In performing the deformation of the k contour a saddle point k_s is encountered where

$$\left.\frac{\partial\Omega}{\partial k}\right|_{k_s} = 0, \quad \Omega_i(k_s) > 0. \quad (2)$$

This is the condition of the so-called pinch singularity. The solution is seen by the observer to be unstable having asymptotic form

$$\psi(x, z, t) = b(k_s)\psi_{k_s}(z)t^{-1/2}e^{-i\Omega(k_s)t} = b(k_s)\psi_{k_s}(z)t^{-1/2}e^{i[k_s x-\omega(k_s)t]}. \quad (3)$$

In particular, if such a saddle point is found for $U = x/t = 0$ with associated $\Omega_i(k_s) > 0$ then the system is absolutely unstable with the perturbation envelope at the point of excitation growing as $\exp[\Omega_i(k_s)t]$. In general, the exponent of the local envelope growth for any x/t is

$$\nu_i = \omega_i(k_s) - \mathrm{Im}(k_s)\frac{x}{t}. \quad (4)$$

Examination of the dispersion relation $\Delta(k, \omega) = 0$ reveals that deformation of the k contour results in the associated ω moving in the complex plane. Because of this, the above procedure is visualized best by examining contour plots of complex ω in the complex k plane. Absolute instability, for instance, would exist if for $x/t = 0$ there is a saddle in ω between the real k axis and the $\omega_i = 0$ contour.

The pulse shape is found by plotting ν_i against x/t. ν_i is proportional to the log of the envelope magnitude and x/t to the horizontal extent, with proportionality factor t_0, the time at which the snapshot is taken.

The pinch singularity method is equivalent to the method of steepest descent and extends the stationary phase technique for stable-wave packets to the complex plane. For absolute instability one would naïvely expect that the region in k space near where the real group velocity vanishes $\partial\omega_r/\partial k_r = 0$ would make the greatest contribution, but this expectation must be modified by taking into account the imaginary parts of ω and k as (2) is the complete condition. We will find that for the Charney problem the real group velocity zero points closely approximate the absolute instability real wavenumber. The basic reason for this is that the growth rates are not so large or rapidly varying with wavenumber as to swamp the real dispersive contribution to the saddle point asymptotics and insofar as these growths are typical we can expect this to be true for other realistic models.

Model flows examined in the past have often been characterized by dispersion relations of the form

$$\omega = kU + ig(k), \quad (5)$$

with U and g real and U constant, so that $\partial\omega_r/\partial k_r = U$ is also constant for all unstable k. The wavenumber selection is in terms of the imaginary variation of ω and the k of largest $g(k)$ will dominate. Models of this type include the two-level model on an f-plane and the Eady model. Insight can be gained by expanding the leading order terms in (5) about $\delta = (x/t) - U$ to obtain an approximate asymptotic pulse (Benjamin, 1961)

$$\psi \approx \exp\left\{i\left(\frac{x}{t} - U\right)k_m t + \left[g(k_m) - \frac{\left(\frac{x}{t} - U\right)^2}{2|g''(k_m)|}\right]t\right\}. \quad (6)$$

where k_m is chosen so that

$$\left.\frac{\partial g}{\partial k}\right|_{k_m} = 0.$$

Absolute instability is predicted in this approximation when the Gaussian wave packet spreads more rapidly than it advects. The limits of the packet are at

$$\frac{x}{t} = U \pm [2g(k_m)|g''(k_m)|]^{1/2}. \tag{7}$$

In these cases the group velocity is constant and the spreading of the packet is determined by the magnitude of the maximum growth rate $g(k_m)$ and the packet width, proportional to $|g''|_{k_m}$. The point of maximum growth, which is the peak of the wave packet, moves at velocity U and has the wavenumber of the most unstable normal mode. Note that the phase speed is also U so that the high or low located at the peak of the packet remains there as the packet propagates. This would not be true for dispersive waves where individual highs and lows move through the packet maximum (Merkine and Shafranek, 1980). Returning to (7), if $x/t < 0$, then absolute instability is predicted by this approximation and the saddle point asymptotics will, in general, confirm this.

The Eady problem with $U(0) = 0$ has a dispersion relation of the form (5). For infinite meridional scale it is

$$\omega = \frac{k}{2} \pm i\left[k \coth k - \frac{k^2}{4} - 1\right]^{1/2}.$$

Evaluation of (7) suggests that this problem just fails to be absolutely unstable (see Appendix). The asymptotic pulse is shown in Fig. 1a. Real wavenumber k_r, imaginary wavenumber k_i, and rest frame frequency, ω_r across the pulse are shown in Fig. 1b. Analytic results for the immediate neighborhood of $x/t = 0, 1$ confirm that $\lim_{x/t \to 0,1} \nu_i = 0$ and that $\lim_{x/t \to 0,1} k_r = \infty$ (Simmons and Hoskins, 1979). If the meridional scale is not infinite ($l \neq 0$) this problem fails to be even marginally absolutely unstable.

In the two-layer model with $\beta \neq 0$, the dispersion relation can be written

$$\omega = k - \frac{\beta}{k}\frac{k^2 + 1}{k^2 + 2} \pm \frac{[\epsilon^2 k^4 (k^4 - 4) + 4\beta^2]^{1/2}}{2k(k^2 + 2)},$$

where ϵ, the shear parameter, is such that the upper layer flow is $U_1 = 1 + (\epsilon/2)$, while the lower layer flow is $U_2 = 1 - (\epsilon/2)$.

The dispersion for real k is shown along with the group speed in Figs. 2a and b for a choice of parameters $\epsilon = 2.0$, $\beta = 1.0$, which result in absolute instability (Merkine and Shafranek, 1980, Fig. 22). The growth rate ν_i from (4) is plotted in Fig. 2c and

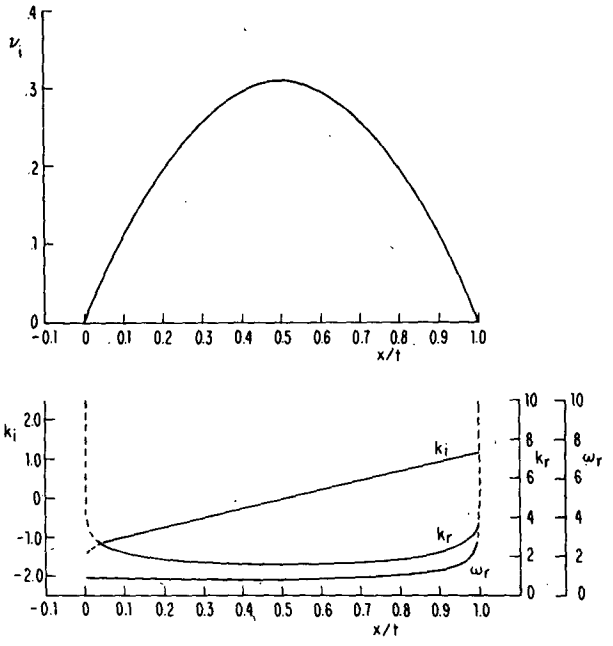

FIG. 1. (a) Local pulse growth rate ν_i as a function of reference frame velocity x/t for the Eady example. Multiplied by any time, t_0, these axes become log of pulse amplitude as a function of distance from the origin of the disturbance. (b) Complex wavenumbers k_r and k_i together with real rest frame frequency ω_r across the pulse in (a).

the local wavenumber across the pulse in Fig. 2d. Note that even though $c_g = \partial w_r/\partial k_r > 0$ for all unstable k, the absolute instability is made up of wavenumbers with lower values of c_g.

Qualitatively speaking, the growth rate is small enough that the effect contained in (6) is dominated near the absolute instability by the tendency of zero, or, as in this case, the smallest available, group velocity waves to make up the stationary part of the instability. This effect is even more striking in the examples that follow, where group velocity zero is associated with appreciable growth rate.

Note that these pulses have finite upstream velocity so that the addition of a sufficiently large uniform zonal velocity to the basic flow would make the absolute instability convective and the same pulse would then be interpreted as a spatially amplifying packet. The fact that the observed zonal surface winds are small and westerly suggests that the atmosphere may often be near an absolute instability state. Of course if zonal surface winds were easterly, absolute instability would be much more common in occurrence and even the Eady problem with $U(0) = 0$ would exhibit absolute instability.

3. The Charney problem

The Charney problem describes quasi-geostrophic perturbations of a zonal flow with velocity a linear

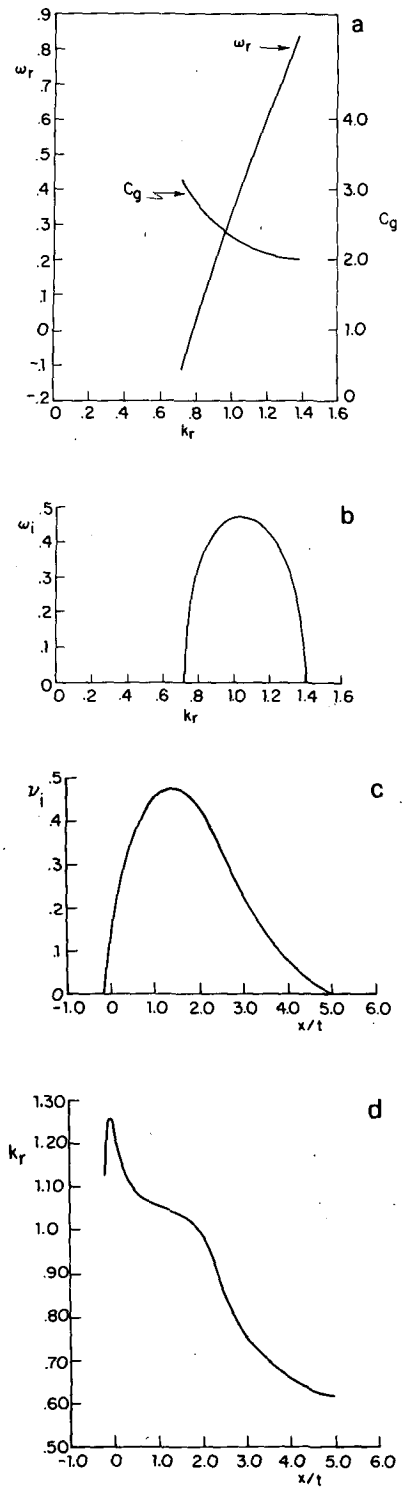

FIG. 2. (a) Nondimensional real frequency ω_r and group velocity c_g as a function of nondimensional wavenumber k_r for the two-level model with $\beta = 1.0$ and $\epsilon = 2.0$. (b) Growth rate ω_i as a function of wavenumber k_i for the example in (a). (c) Local pulse growth rate ν_i as a function of reference frame velocity x/t for the example in (a). Multiplied by any time t_0, these axes become log of pulse amplitude as a function of distance from the origin of the disturbance. (d) Real wavenumber k_r across the pulse in (c).

function of height only, $U(z) = mz$. The scale height H and Brunt-Vaisala frequency N are constant. The effects of sphericity are confined to the β-plane approximation. In what follows, the notation of Lindzen *et al.* (1980) will be used.

Conservation of pseudo-potential vorticity requires for the stream function Ψ

$$\psi_{zz} + \left\{\frac{q(y)}{U-c} - \frac{\alpha^2}{\epsilon} - \frac{1}{4H^2}\right\}\psi = 0, \tag{8}$$

where

$\Psi = \psi(z)e^{z/2H}e^{ik(x-ct)}e^{ily}$
$\alpha^2 = k^2 + l^2$, the sum of square zonal and meridional wavenumbers
$q(y) = (\beta/\epsilon) + (U_z/H) - U_{zz}$
$H = RT_0/g$, the scale height
$\epsilon = f^2/N^2$
f = Coriolis parameter
$\beta = \partial f/\partial y$
x = distance in eastward direction
y = distance in northward direction
z = height.

The boundary condition requires that the vertical velocity vanish at the ground, i.e.,

$$\psi_z + \frac{\psi}{2H} - \frac{U_z}{U-c}\psi = 0, \quad z = 0, \tag{9a}$$

and that ψ approach zero at infinity

$$\lim_{z\to\infty} \psi(z) = 0. \tag{9b}$$

We assume a linear shear $U(z) = mz$, and make the following nondimensionalizations

$$\tilde{U} = U/mH, \quad \tilde{z} = z/H,$$
$$\tilde{c} = c/mH, \quad \tilde{\alpha}^2 = \alpha^2 H^2/\epsilon,$$

so that (8) and (9) become

$$\psi_{\tilde{z}\tilde{z}} + \left(\frac{r+1}{\tilde{z}-\tilde{c}} - \delta^2\right)\psi = 0, \tag{10}$$

$$\psi_{\tilde{z}} + \frac{\psi}{2} + \frac{\psi}{\tilde{c}} = 0, \quad z = 0, \tag{11a}$$

$$\lim_{z\to\infty} \psi(\tilde{z}) = 0, \tag{11b}$$

where

$$r = \beta H/\epsilon m,$$
$$\delta^2 = \tilde{\alpha}^2 + 1/4 = \tilde{k}^2 + \tilde{l}^2 + 1/4. \tag{12}$$

For typical midlatitude values of constants we have

$$\beta = 1.6 \times 10^{-11}\ \text{s}^{-1}\ \text{m}^{-1}$$
$$H = 8 \times 10^3\ \text{m}$$
$$\epsilon = 0.625 \times 10^{-4}$$
$$m = 2.05 \times 10^{-3}\ \text{s}^{-1}$$
$$r = 1.0$$

so that $\tilde{k}$ is related to dimensional wavelength by

$$\lambda = \frac{2\pi H}{\sqrt{\epsilon}} \frac{1}{\tilde{k}} = \frac{6.4 \times 10^6 \text{ m}}{\tilde{k}}. \tag{13}$$

The tildes are dropped in the following.

The analysis of pinch singularities outlined above requires a dispersion relation $\Delta(\omega, k)$ valid in the complex k and ω planes. In principle, the eigenproblem (10, 11) could be solved repeatedly to obtain these eigenvalues but the computational burden would be large. Fortunately, Lindzen and Rosenthal (1981) recently obtained a highly accurate WKB solution for the baroclinic problem, which is valid in the complex plane. Their dispersion relation takes the form

$$\left\{\frac{1}{2} + \frac{k}{\omega} - \left[\frac{1}{2x(\omega/k)}\left(\delta^2 + \frac{r+1}{\omega/k}\right)^{1/2} + \frac{1}{4}\frac{r+1}{(\omega/k)^2}\left(\delta^2 + \frac{r+1}{\omega/k}\right)^{-1}\right]\right\}$$
$$\times \left\{-2\sin(\pi - z_T)e^{-i(\pi - z_T)}K_1\left[x\left(\frac{\omega}{k}\right)\right] + I_1\left[x\left(\frac{\omega}{k}\right)\right]\right\}$$
$$- \left(\delta^2 + \frac{r+1}{\omega/k}\right)^{1/2}\left\{\frac{-2\sin(\pi - z_T)}{\pi} e^{-i(\pi - z_T)}K_1'\left[x\left(\frac{\omega}{k}\right)\right] + I_1'\left[x\left(\frac{\omega}{k}\right)\right]\right\} = 0,$$

where

$$z_T = \pi(r+1)/2\delta,$$

$$x\left(\frac{\omega}{k}\right) = \frac{\omega}{k}\left(\frac{r+1}{\omega/k} + \delta^2\right)^{1/2}$$
$$+ \frac{r+1}{\delta}\ln\left\{\left(\frac{\omega/k}{r+1}\right)^{1/2}\left[\delta + \left(\frac{r+1}{\omega/k} + \delta^2\right)^{1/2}\right]\right\}.$$

Nine term expansions of the Bessel functions were used and the real k dispersion relation obtained for a representative midlatitude value of the stability parameter $r = 1$. The real k dispersion relation for meridional wavenumber $l = 0$ is shown in Figs. 3a and 3b. Real group velocity zero can be estimated at $k \simeq 6$ and $k \simeq 0.7$. Associated saddle points in the complex plane are shown in Fig. 4a and, with more detail in the region near $k = 0.7$, in Fig. 4b. Contributions to the asymptotic solution for absolute instability come from these points which can be found to lie at (nondimensional) $k = 5.69\text{-}2.93i$, and $k = 0.666\text{-}0.113i$.

The wavenumber of maximum growth predicted by normal mode analysis is $k_N = 1.4$. Corresponding

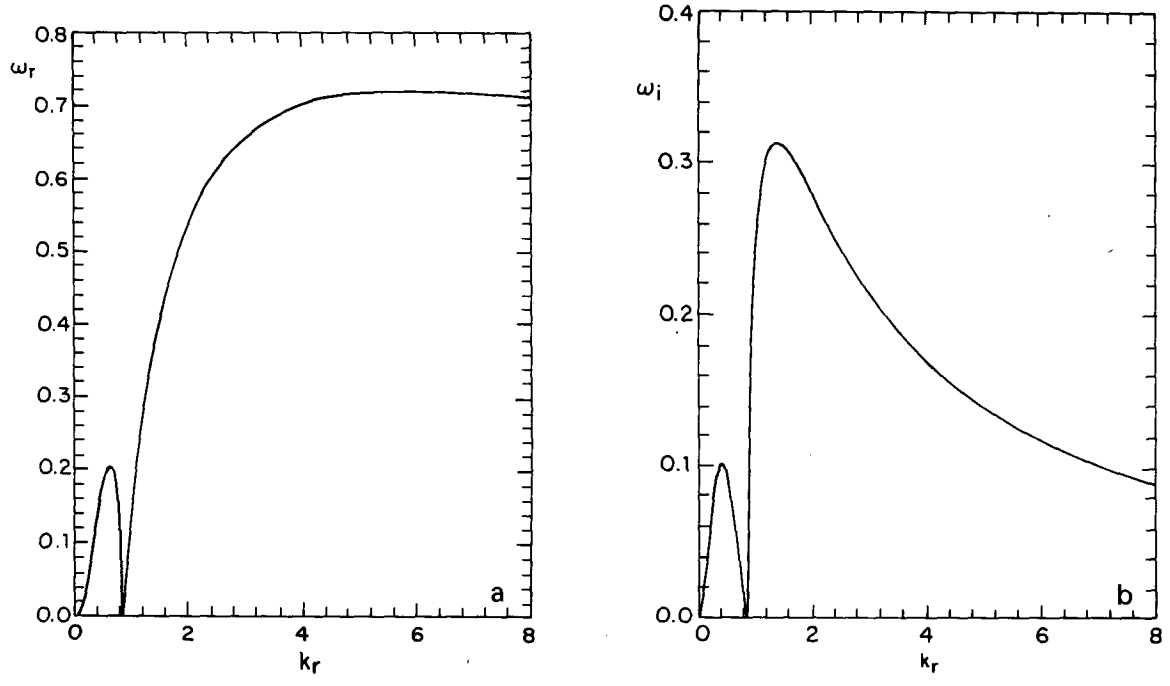

FIG. 3. (a) Nondimensional real frequency ω_r as a function of nondimensional real wavenumber k_r for the Charney problem with $r = 1.0$. (b) Nondimensional imaginary frequency ω_i as a function of real wavenumber k_r for $r = 1.0$.

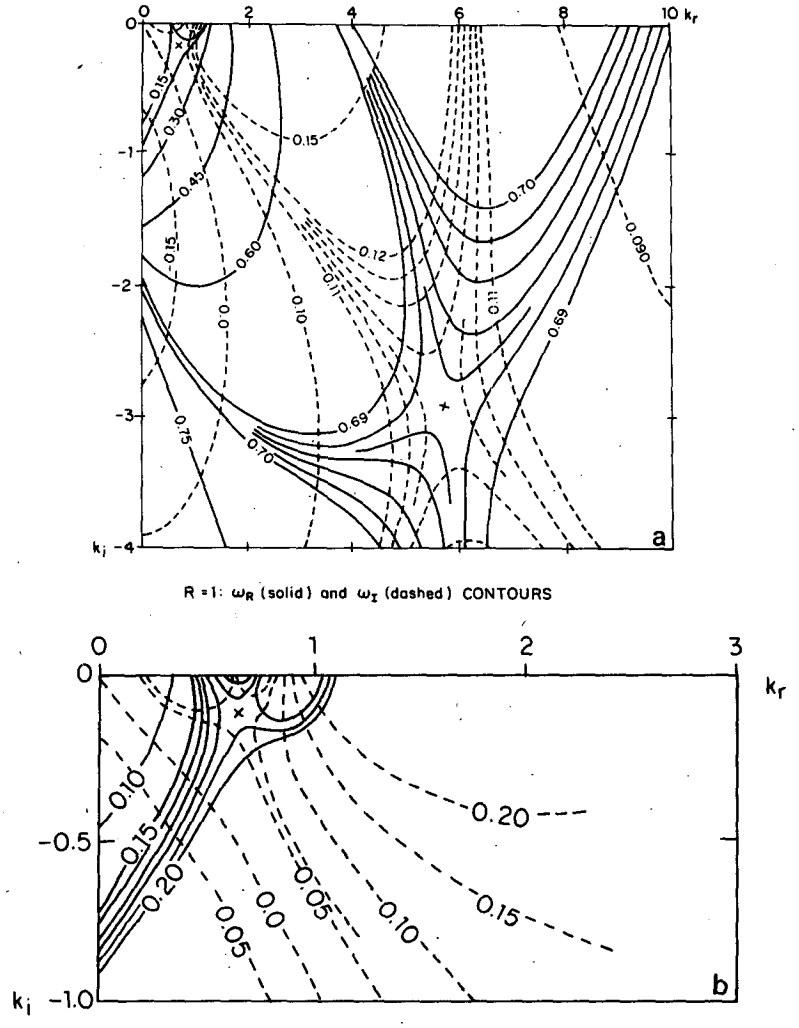

FIG. 4. (a) The complex dispersion relation for the Charney problem with $l = 0$ and $r = 1.0$. Shown are contours of ω in the k plane. Full lines are constant ω_r, dashed lines are constant ω_i. (b) As in (a) except detail for saddle near $k = 0.67$.

dimensional wavelength calculated from (13) are: $\lambda_N = (6.4 \times 10^6)/1.4\ m = 4600$ km for the normal mode and $\lambda_a = (6.4 \times 10^6)/5.69\ m = 1120$ km for the absolute instability. The latter compares favorably with observed scales of cyclogenesis (Buzzi and Tibaldi, 1978; Reed, 1979).

Because these saddle points are separated in scale and arise from distinct regions of the dispersion relation—the first from the Charney mode and the second from the Burger mode—it is instructive to derive the pulse asymptotics separately. The dominant mode for any x/t can be quickly determined by comparison if desired.

Fig. 5a shows the pulse shape for the saddle located in the Charney mode. Wavenumber and frequency across the pulse are shown in Fig. 5b. Note that ω_r is the rest frame frequency which is related to the local frequency by $\nu_r = \omega_r - k_r(x/t)$.

High wavenumbers are found in the vicinity of the origin of the disturbance with the leading edge of the pulse being made up of wavenumbers near the neutral point in the dispersion at $k = 0.87$ where the real group velocity is at a maximum. Phase speeds of the short waves making up the absolute instability are small. Downstream, the wavelength rises until at the pulse peak we recover the maximum growth rate normal mode at $k = 1.4$. We note that this increase in wavelength has been found in other β-plane models as well (Simmons and Hoskins, 1979) and appears to be a quite general feature. Further downstream, the pulse shape is dependent on the detail of the dispersion in the neighborhood of the neutral point with the leading edge dominated by the longest waves near $k = 0.87$. Upstream influence shows a rapid decay in space with k_i large and negative.

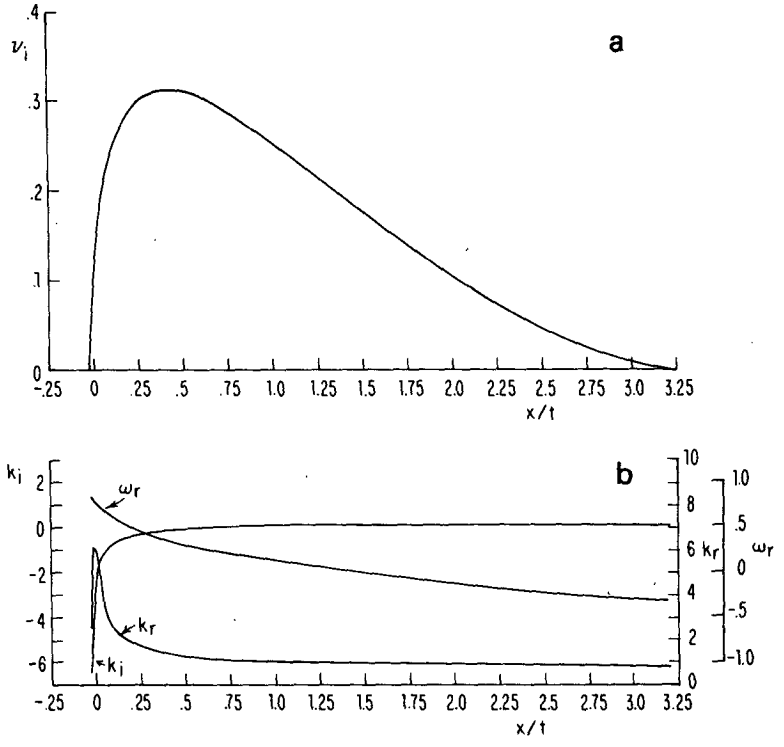

FIG. 5. (a) Local pulse growth rate ν_i arising from the saddle point in the Charney mode for $l = 0$, $r = 1.0$, as a function of reference frame velocity x/t. Multiplied by any time t_0, these axes become log of pulse amplitude as a function of distance from the origin of the disturbance. (b) Complex wavenumbers k_r and k_i together with real rest frame frequency ω_r across the pulse in (a).

The pulse arising from the Burger mode is shown in Figs. 6a and 6b. The growth rate is smaller than the Charney, but nonetheless dominates the upstream influence. Upstream influence is characterized by the high negative group velocity waves and downstream by the positive with the absolute instability located near the zero of group velocity.

So far only perturbations infinite in the meridional direction, corresponding to $l = 0$ have been considered. The saddle point method can be generalized to

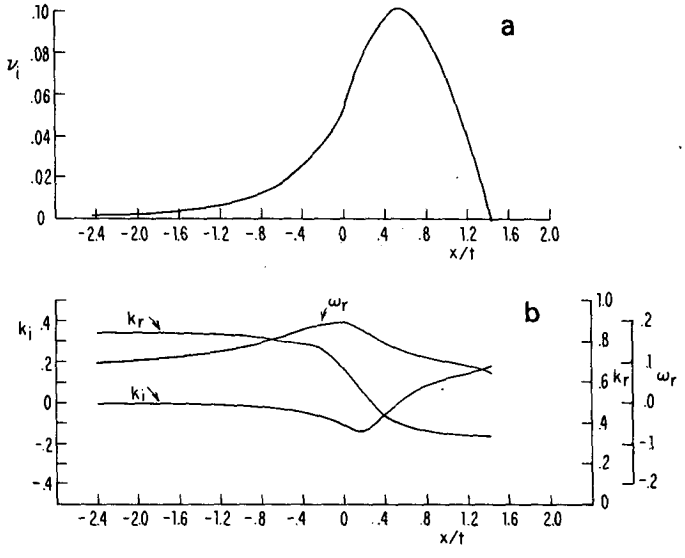

FIG. 6. As in Fig. 5 except for the saddle point in the Burger mode.

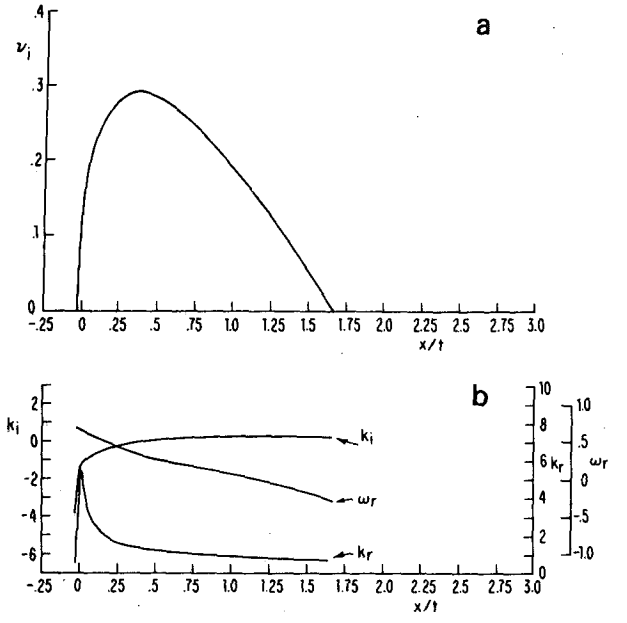

FIG. 7. As in Fig. 5 except for $l = 1/2$.

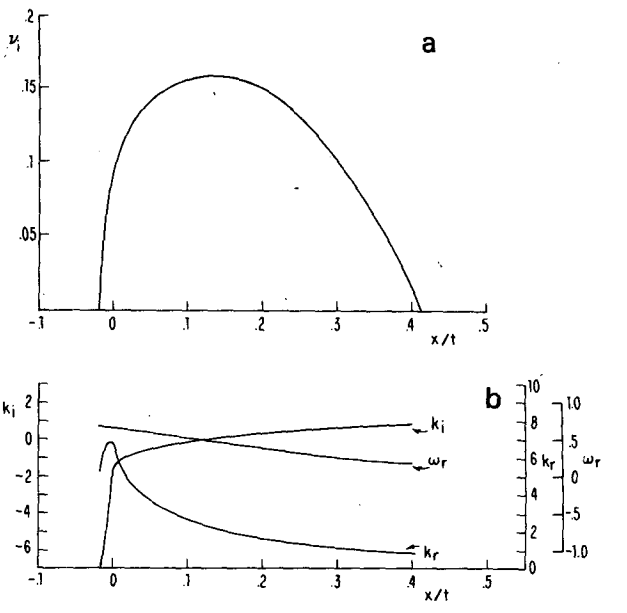

FIG. 9. As in Fig. 5 except for $l = 2$.

two or more dimensions (Bers, 1975), but these solutions present many difficulties. In fact, the initial perturbation is likely to be a distributed source of vorticity and problems associated with point sources in two and three dimensions do not necessarily yield insight commensurate with these difficulties. The simplest localized source to use is the fundamental mode in a channel, and taking this to be 6400 km wide, we choose $l = 1/2$ in the expression for δ^2 (12).

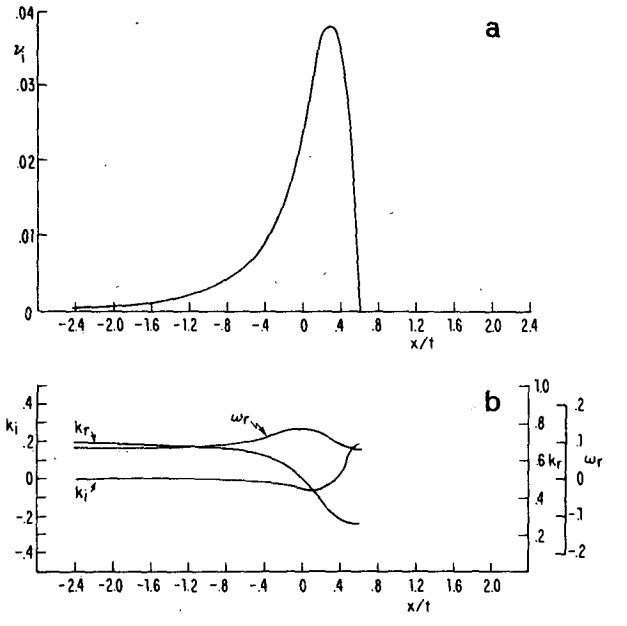

FIG. 8. As in Fig. 5 except for Burger mode saddle and $l = 1/2$.

The Charney absolute instability point moves to $k = 5.77 - 2.87i$; $\omega = 0.692 + 0.112i$, and the absolute instability point associated with the Burger mode moves to $k = 0.516 - 0.059i$; $\omega = 0.137 + 0.205i$. The pulse arising from the former is shown in Fig. 7a and associated quantities in Fig. 7b. The pulse from the Burger mode is shown in Figs. 8a and 8b. We remark that the general features discussed above for the $l = 0$ case persist, but the detail of the leading edge is modified. This effect is even more pronounced when the meridional wavenumber is further restricted to $l = 2$, corresponding to a channel width of 1600 km. The Charney mode pulse survives and is shown in Figs. 9a and 9b. Absolute instability occurs for $k = 6.98 - 2.25i$ and $\omega = 0.675 + 0.090i$. The maximum growth rate at $k = 2.19$ is only 1.74 times the absolute instability growth rate. What is even more remarkable is that the growth of an individual disturbance will be significantly larger than this would indicate, at least near the absolute instability point. This is because the local growth depends also on the wave phase speed in relation to the local pulse speed and the derivative of growth with local pulse speed (Simmons and Hoskins, 1979)

$$\hat{\nu}_i = \nu_i\left(\frac{x}{t}\right) + \left(c_r - \frac{x}{t}\right)\frac{\partial \nu_i}{\partial(x/t)}. \qquad (14)$$

This effect enhances the apparent growth of waves between the origin and the peak of the pulse. The phase and group velocity difference is shown in Fig. 10; we can evaluate (13) for $x/t = 0.0$ to find

$$\hat{\nu}_i \approx 0.09 + (0.1)(2.0) = 0.29.$$

The apparent growth is nearly twice as fast as the maximum growth rate normal mode and with a wavenumber considerably higher being $k \approx 7.0$, resulting in a dimensional wavelength from (13) of $\lambda = 920$ km, which is a reasonable scale for the early stages of cyclogenesis (Reed, 1979). Remarkably, individual waves at the leading edge of the pulse can be seen to exceed maximum normal mode growth rates as well.

When making connection with more detailed models it must be borne in mind that the presence of a jet structure in the meridional often effectively limits the wave to smaller meridional scales than the geometric constraint alone would imply. Consequently this $l = 2$ case compares most closely with primitive equation integrations with realistic jets (Simmons and Hoskins, 1979).

4. Discussion

Absolute instability, previously found in the two-level models (but absent in the Eady problem), has been confirmed to exist in the Charney problem.

Examination of the dispersion relation for zeros of real group velocity allows a useful estimate to be made of the wavenumber characterizing the absolute instability.

Because decrease of phase speed with increasing wavenumber is a robust feature of more realistic dispersion relations (Geisler and Garcia, 1977; Simmons and Hoskins, 1976), it is suggested that the high wavenumber, low phase speed and rapid growth found for the absolute instability here may be a quite general feature.

This result of short initial scales maturing into larger scales and possessing high growth rate encourages the identification of absolute instability with preferred regions of cyclogenesis (Merkine, 1977; Buzzi and Tibaldi, 1978), and the low phase speed at least partially answers the objection of Simmons and Hoskins (1979) that the individual low may propagate out of the region of enhanced baroclinicity before obtaining substantial amplitude.

In normal mode analysis it is generally assumed that the basic state is either zonally unbounded or periodic and a function only of height and latitude. Such uniformity is not found in the atmosphere where regions of enhanced baroclinicity result in preferred areas for cyclogenesis (Petterssen, 1956). The absolutely unstable waves described here would be able to take advantage of these inhomogeneous states by virtue of their small scale and rapid growth coupled with low-phase speed. As has been noted, the predicted wavelengths of the absolute instability are commonly observed even though they are much shorter than those suggested by normal mode analysis.

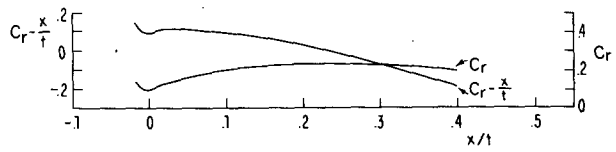

FIG. 10. Rest frame phase speed c_r and apparent phase speed as viewed from the translating frame $c_a = c_r - x/t$ for the case in Fig. 9a.

The two-level and Eady models are limited by unrealistically high phase speeds, with steering levels near the center of the flow, and by the lack of a potential for zero group velocity. It would seem that the Charney problem is the simplest model that produces the observed scales.

The asymptotics of long waves which in the Charney model arise from the Burger mode were separately derived above. While the Charney mode waves in general dominate, at least in the downstream solutions, the separation in scale between the waves making up these pulses suggests that observational correlates may be found for both. In particular, the variation of the dispersion as the zonal velocity and Brunt-Vaisala frequency change, say from continental land masses to ocean or in time, may result in the absolute instability being manifest in one or the other modes separately.

It is of interest to note that the amplitude and scale of waves in the atmosphere often behave as would be expected from the above pulse asymptotics, e.g., Sanders and Gyakum (1980, their Fig. 7). Here, two areas of origin of the wave envelope may be identified: in the Atlantic off the east coast of the United States and in the Pacific near Japan. The episodic occurrence of absolute instability in these jet entrance regions could result in the observed index cycle variations noted downstream from them (Nitta and Yamamoto, 1973).

These considerations imply that an accurate forecast model must closely approximate the dispersive properties of unstable waves over the entire range of wavenumbers making significant contributions to the asymptotic pulse; it is not sufficient to do well near the wavenumber of the most rapidly growing normal mode. Conversely, having an accurate local linear dispersion relation, either for the atmosphere or a model simulation, it should be possible to predict regions of cyclogenesis and the scales, phase speeds and growth rates of the unstable waves. Initially, the scale can be approximated by the wavenumber of zero group velocity, which can be easily found from the common phase speed vs. wavenumber plot by noting that the group velocity is given by

$$c_g = \frac{\partial \omega_r}{\partial k_r} = \frac{\partial k_r c}{\partial k_r} = c + k_r \frac{\partial c}{\partial k_r},$$

where $c = \omega_r / k_r$ is the phase speed.

Application to the 30° jet of Simmons and Hoskins (1976) predicts absolute instability ($c_g = 0$) for zonal wavenumber $\sim$ 16. Realistic results for spectral models would require a truncation that not only generously includes this wavenumber but also has a realistic dispersion relation at these small scales as well.

5. Relation to blocking ridge development

The central North Pacific and North Atlantic are preferred locations for the development of planetary-scale stationary perturbations in the zonal geopotential height field. These so-called blocks have been well documented in the literature but their origin remains a matter of controversy. Recently a mechanism for the growth and maintenance of planetary waves by the interaction between cyclone-scale waves and the mean flow has been identified in a GCM simulation. (Gall and Blakeslee, 1979). Essentially, the ultralong waves result from spontaneously occurring inhomogeneities in the amplitude of the cyclone scale waves. While their model generates the inhomogeneity internally from a zonally uniform jet, it is at least as likely that zonal inhomogeneity in the jet would give rise to similar effects. In particular, the occurrence of an absolute instability in the jet would be revealed by an outlining stationary envelope of planetary scale, with the upstream edge of the block being coincident with the absolute instability point in the zonally varying jet. Because absolute instability generates weak upstream velocity, it would be expected that the occurrence of blocks should be highly correlated with weak upstream jets. Such a correlation is observed (White and Clark, 1975; their Fig. 12), (Wallace and Gutzler, 1981; their Fig. 21), with the frequency of blocking increasing when zonal average surface winds drop below $\sim$3 m s^{-1}. Note that while the Charney problem dispersion (Fig. 9a) gives maximum dimensional upstream velocity

$$\left(\frac{x}{t}\right)_{\text{dim}} = 0.02mH = 0.33 \text{ m s}^{-1}.$$

This number is sensitive to the shear, m and to the details of the dispersion relation near the wavenumber of absolute instability, as can be seen by examining the pulse in Fig. 6a which exhibits much higher upstream velocities.

A quantitative test of this mechanism could be made by calculating the dispersion relation in the jet region and correlating the occurrence of absolute instability with blocking (in a first approximation looking for $c_g = 0$).

Acknowledgments. The author wishes to thank Dr. R. S. Lindzen for his helpful criticism, Dr. Arthur Rosenthal for kindly checking the approximations and lending his computer graphics expertise and Dr. R. Pierrehumbert for introducing him to the concept of absolute instability. This work was supported by NASA Grant NGL-22-007-228.

APPENDIX

Benjamin's Approximation Applied to the Eady Problem

The dispersion relation for Eady's model can be written in the form (5)

$$\omega = \frac{k}{2} \pm i\left(k \coth k - \frac{k^2}{4} - 1\right)^{1/2},$$

$$U = 1/2,$$

$$g = \pm\left(k \coth k - \frac{k^2}{4} - 1\right)^{1/2}.$$

The maximum of g, $g(k_m) = 0.310$, occurs at $k_m = 1.6062$. (5) can be evaluated as

$$g^2 = k \coth k - \frac{k^2}{4} - 1,$$

$$(g^2)'' = 2(g'^2 + gg'')$$

$$= 3/2 + 2 \coth k(k \coth^2 k - \coth k - k),$$

$$g''|_{km} = \frac{3/4 + \coth k_m(k_m \coth^2 k_m - \coth k_m - k_m)}{g(k_m)}$$

$$= 0.389,$$

so that the limits of the packet are predicted to occur at

$$\frac{x}{t} = \frac{1}{2} \pm [2g(k_m)|g''|_{k_m}]^{1/2} = \frac{1}{2} \pm 0.491 > 0,$$

suggesting that this flow just fails to achieve absolute instability.

REFERENCES

Benjamin, T. B., 1961: The development of three-dimensional disturbances in an unstable film of liquid flowing down an inclined plane. *J. Fluid Mech.*, **10**, 401–419.

Bers, A., 1975: Linear waves and instabilities. *Physique de Plasmas*, C. DeWitt and J. Peyrand, Eds., Gordon and Breach, 157–183.

Briggs, R. J., 1964: *Electron-Stream Interaction with Plasmas.* MIT Press, pp. 8–46.

Burger, A. P., 1966: Instability associated with the continuous spectrum in a baroclinic flow. *J. Atmos. Sci.*, **23**, 272–277.

Buzzi, A., and S. Tibaldi, 1978: Cyclogenesis in the lee of the Alps: A case study. *Quart. J. Roy. Meteor. Soc.*, **104**, 271–287.

Charney, J. G., 1947: The dynamics of long waves in a baroclinic westerly current. *J. Meteor.*, **4**, 135–162.

Eady, E. T., 1949: Long waves and cyclone waves. *Tellus*, **1**, 33–52.

Farrell, B. F., 1982: The initial growth of disturbances in a baroclinically unstable flow. Submitted to *J. Atmos. Sci.*

Gall, R., and R. Blakeslee, 1979: Cyclone-scale forcing of ultralong waves. *J. Atmos. Sci.*, **36,** 1692–1698.

Geisler, J. E., and R. Garcia, 1977: Baroclinic instability at long wavelengths on a β-plane. *J. Atmos. Sci.*, **34,** 311–321.

Lindzen, R. S., Brian Farrell and Ka-Kit Tung, 1980: The concept of wave overreflection and its application to baroclinic instability. *J. Atmos. Sci.*, **37,** 44–63.

——, and A. J. Rosenthal, 1981: A WKB asymptotic analysis of baroclinic instability. *J. Atmos. Sci.*, **38,** 619–629.

Merkine, L.-O., 1977: Convective and absolute instability of baroclinic eddies. *Geophys. Astrophys. Fluid Dyn.*, **9,** 129–157.

——, and M. Shafranek, 1980: The spatial and temporal evolution of localized unstable baroclinic disturbances. *Geophys. Astrophys. Fluid Dyn.*, **16,** 175–206.

Nitta, T., and J. Yamamoto, 1973: A diagnosis of the formation of intermediate scale disturbances near Japan; the western Pacific and Southeast Asia. *Pap. Meteor. Geophys.*, **24,** 289–309.

Petterssen, S., 1956: *Weather Analysis and Forecasting,* Vol I. McGraw-Hill, 428 pp.

Reed, R. J., 1979: Cyclogenesis in polar air streams. *Mon. Wea. Rev.*, **107,** 38–52.

Sanders, F., and J. R. Gyakum, 1980: Synoptic-dynamic climatology of the "bomb." *Mon. Wea. Rev.*, **108,** 1589–1606.

Simmons, A. J., and B. J. Hoskins, 1976: Baroclinic instability on the sphere: Normal modes of the primitive and quasi-geostrophic equations. *J. Atmos. Sci.*, **33,** 1454–1477.

——, and ——, 1979: The downstream and upstream development of unstable baroclinic waves. *J. Atmos. Sci.*, **36,** 1239–1254.

Wallace, J. M., and D. S. Gutzler, 1981: Teleconnections in the geopotential height field during the Northern Hemisphere winter. *Mon. Wea. Rev.*, **109,** 784–812.

White, W. B., and N. E. Clark, 1975: On the development of blocking ridge activity over the central North Pacific. *J. Atmos. Sci.*, **32,** 489–502.